SUPPLEMENTARY INFORMATION

Supplementary Materials and Methods

Supplementary Figures

Supplementary Tables

Supplementary References

Supplementary Materials and Methods

Generation of resistant cells

Kasumi-1 and MV4-11 cells were cultured continuously with a step-wise increase of nilotinib concentrations (0.1, 0.3, 0.5, 0.75, 1 µM) for 10 weeks. Cells cultured in parallel without nilotinib were served as parental negative controls. Cells were considered resistant when they could routinely grow in medium containing 1 µM nilotinib. Resistant cells were maintained in medium containing 1 µM nilotinib. Before any further investigations, both resistant and parental cells were growing in the same condition for 96 hours.

Electrophoretic mobility-shift (EMSA) assays

EMSA assays using nuclear extracts and ^{32}P-labeled probes were performed as previously described (1,2). Briefly, DNA oligo probes (sequences in Supplementary Table) derived from the *DNMT1* promoter containing Sp1 binding sites were labeled by ^{32}P-dCTP and Klenow. Nuclear extracts from Kasumi-1 and MV4-11 cells were prepared using the Nuclear and Cytoplasmic Extraction Reagent (Pierce) and incubated with ^{32}P-labeled probes. Electrophoresis was performed by using 6% DNA Retardation Gels (ThermoFisher Scientific).

Wright-Giemsa staining

Approximately 0.5×10^4 bone marrow cells were harvested and cytospun on a slide at 1,000 rpm for 8 min. The slides were air-dried and stained using the Hema-3 Kit (Fisher Scientific) following the protocol described previously (3).

Hematoxylin and Eosin (H&E) staining

Tissues collected from mice were fixed in 10% paraformaldehyde/PBS, paraffin-embedded, and sectioned (5 μm in thickness). H&E staining was performed as previously described (3-5). An image of each tissue section was captured using a Zeiss Axiovert 40 CFL inverted, digital light microscope.

Reporter gene assays

The human *DNMT1* gene promoter region (−1048/+36) containing the Sp1 binding site, 5'-TGGGGGGGGT-3', was cloned into the pGL3 firefly luciferase reporter vector (pGL3-*DNMT1*). 293T cells were transfected with the pGL3-*DNMT1* or *Sp1* expression vector plus the pRL-SV40 Renilla luciferase plasmid (Promega) using the Lipofectamine™ reagent (Life Technologies), and firefly luciferase activity was measured at 48 h post-transfection using a dual luciferase reporter assay system (Promega) as previously described (3-5).

GEO (Gene Expression Omnibus) data analysis

The GEO datasets GSE12417 (6), GSE19567 (7), GEO33075 (8), GSE51083 (9), GDS3518 (10), GDS4177 (11), GDS4175 (11), GDS838 (12) and GDS2706 (13) were analyzed by gene-expression arrays for mRNA expression of *KIT*, *FLT3*, *DNMT1*, *DNMT3a* and *DNMT3b*. The patients reported in these GEO datasets are cytogenetically normal AML, CML or ALL. The detailed clinical characteristics of patients were referred in the original reports. These samples were normalized, managed and analyzed by GraphPad Prism 5 Software.
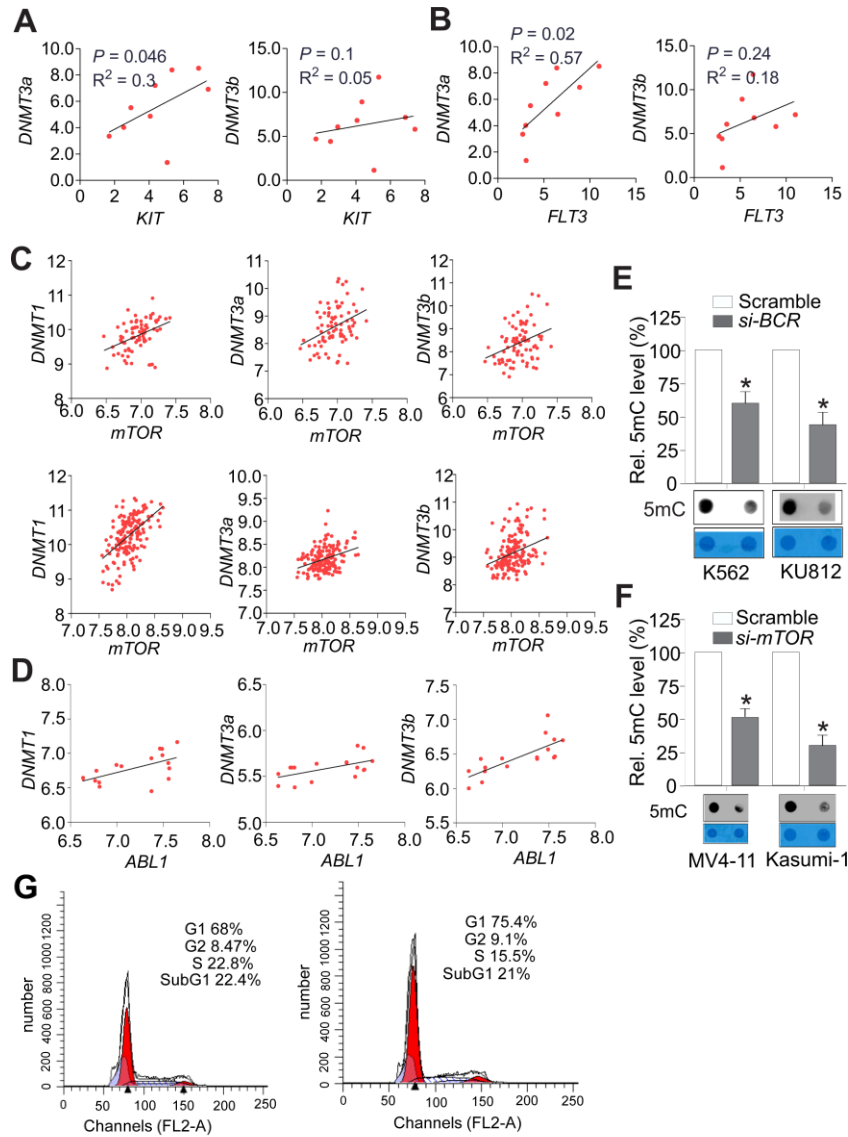
Supplementary Figure 1. Tyrosine kinases are positive regulators of DNMT-dependent DNA methylation in leukemia cells.

A and B, The analysis of qPCR results from 9 leukemia cell lines showing the correlation between *KIT* (**A**) or *FLT3* (**B**) and *DNMT3a or DNMT3b* expression. **C**, The analysis of GSE12417 GPL570 (AML, n = 79, upper) and GSE12417 GPL96 (AML, n = 163, lower) showing the correlation between *mTOR* and *DNMT* expression. **D**, The analysis of GSE5550 GPL201 (CML, n = 17) showing the correlation between *ABL1* and *DNMT* expression. **E**, K562

4

or KU812 cells were transfected with *BCR* siRNA for 48 h, and the genomic DNA was subjected to dotblot analysis using anti-5mC. **F**, MV4-11 or Kasumi-1 cells were transfected with *mTOR* siRNA for 48 h, and the genomic DNA was subjected to dotblot analysis using anti-5mC. **G**, Kasumi-1 cells were transfected with *KIT* siRNA for 48 h and subjected to flow cytometry analysis. In **A-D**, the correlation between *RTKs* and *DNMTs* was assessed by Spearman correlation analysis; in **E** and **F**, the representative images and quantitative graphs indicate DNA methylation levels and data are shown as mean values $\pm$ S.D. from 3 independent experiments, *$P < 0.05$; in **G**, representative data from 3 independent experiments that gave similar results are shown.
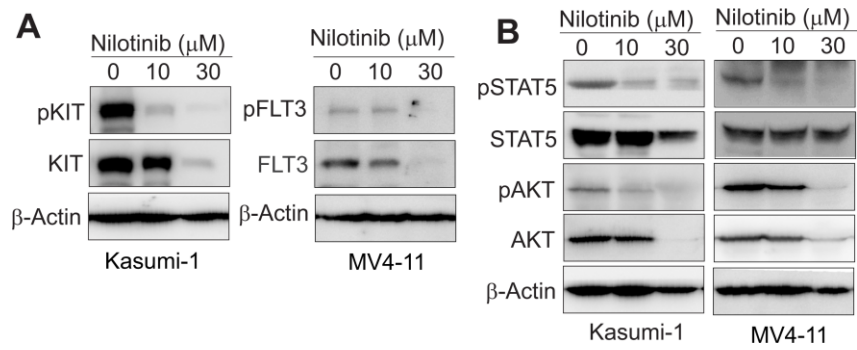
Supplementary Figure 2. Nilotinib treatment inhibits KIT and FLT3 kinase signaling.

A and **B**, Kasumi-1 or MV4-11 cells were treated with nilotinib at concentrations of 10 or 30 μM for 24 h and subjected to Western blot analysis to determine protein expression and phosphorylation levels.
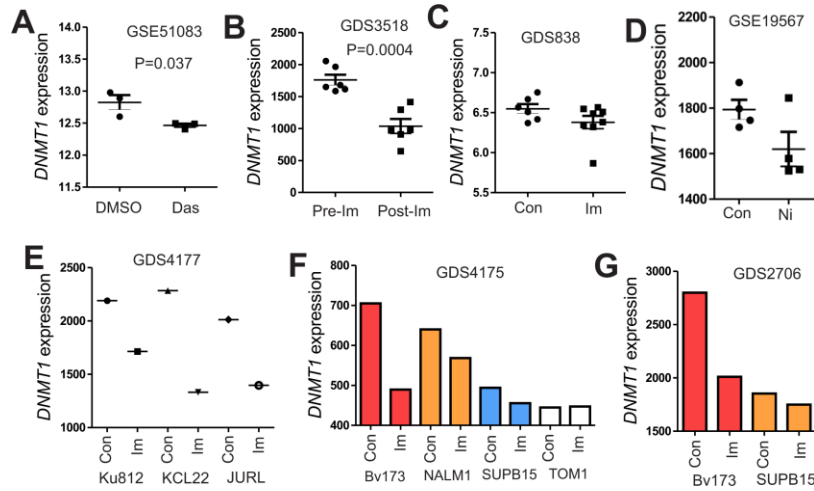
Supplementary Figure 3. Treatment with RTK inhibitors decreases *DNMT1* expression *in vitro* and *in vivo*.

A-**G**, Analysis of multiple GEO datasets for *DNMT1* expression *in vitro* and *in vivo* in the presence or absence of RTK inhibitors. In **B**, the graph shows the 24 h treatment. Con = control; Das = dasatinib; Im = imatinib; Ni = nilotinb.
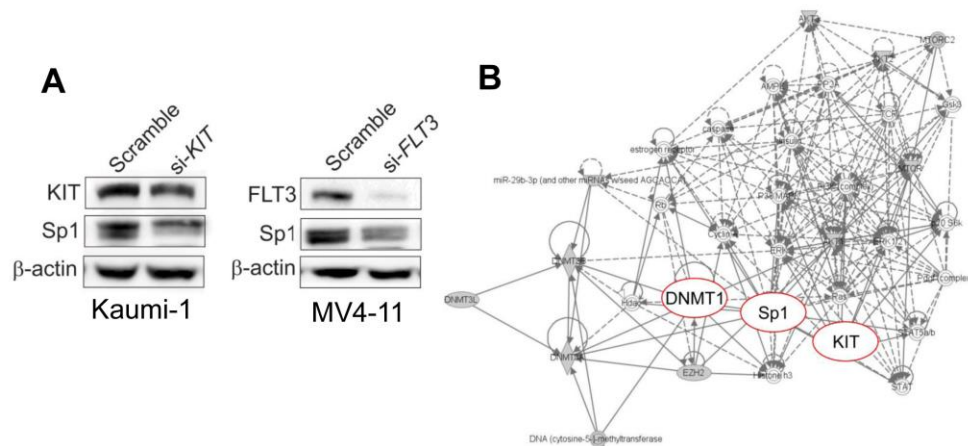
Supplementary Figure 4. The potential biochemical link between an RTK and DNMT1. **A**, Western blot analysis in Kasumi-1 or MV4-11 cells transfected with *KIT* or *FLT3* siRNA or scrambled control, respectively, for 48 hours. Data represent 3 independent experiments. **B**, The genes reported to be under the control of DNMT/RTK pathways were used as input for pathway analysis using the ingenuity pathway analysis (IPA) software. The network shows the interactions among *DNMT1*, *Sp1* and *KIT*.
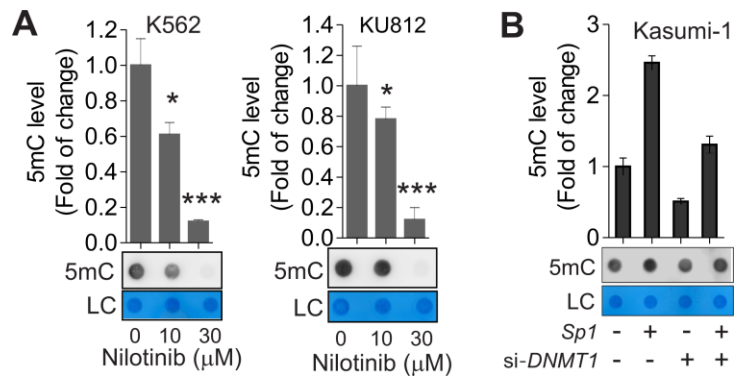
Supplementary Figure 5. Nilotinib treatment induces global and gene specific DNA methylation through the Sp1-DNMT1 axis.

A, K562 and KU812 cells were treated with nilotinib for 48 h and the genomic DNA was subjected to dotblot analysis. **B**, Kasumi-1 cells were transfected with *Sp1* expression vectors for 24 h followed by *DNMT1* siRNA for another 24 h. Genomic DNA was subjected to dotblot analysis. Upper, representative image of dotblotting; lower, the graph shows the quantification of dot intensity. Data are shown as mean values ± S.D. from 3 independent experiments; LC = loading control; *$P < 0.01$, ***$P < 0.001$.
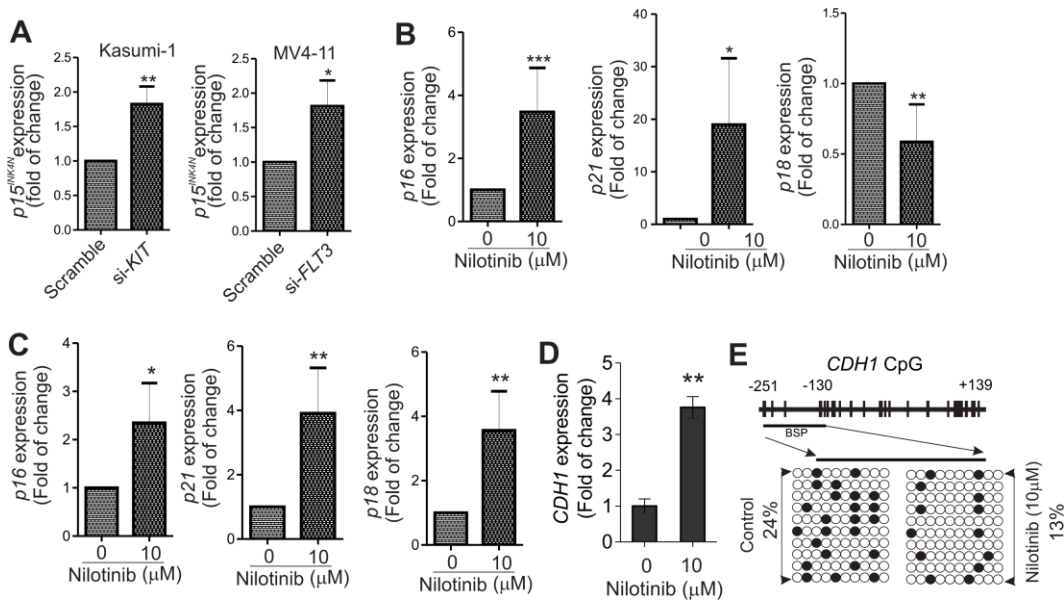
Supplementary Figure 6. RTK dysfunction reactivates cyclin-dependent kinase inhibitors. **A**, qPCR measuring expression of $p15^{INK4B}$ in Kasumi-1 or MV4-11 cells transfected with *KIT* or *FLT3* siRNA or scrambled control for 48 h. **B** and **C**, qPCR for assessing expression of *p16*, *p18* and *p21* in Kasumi-1 (**B**) or MV4-11 (**C**) cells treated with 10 µM nilotinib for 48 h. **D** and **E**, Kasumi-1 cells were treated with nilotinib for 48 h and subjected to qPCR for *CDH1* expression (**D**) or bisulfite sequencing for *CDH1* gene promoter methylation (**E**). Data are shown as mean values ± S.D. from 3 independent experiments; *$P < 0.01$, **$P < 0.01$, ***$P < 0.001$.
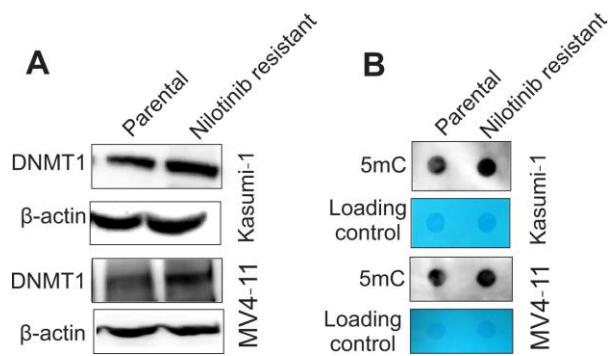
Supplementary Figure 7. DNMT1-dependent DNA methylation is increased in cells resistant to nilotinib. **A**, Western blot to determine the levels of DNMT1 expression in resistant and parental cells. **B**, The genomic DNA was isolated from resistant or parental cells and subjected to dotblot analysis. Data represent 3 independent experiments.
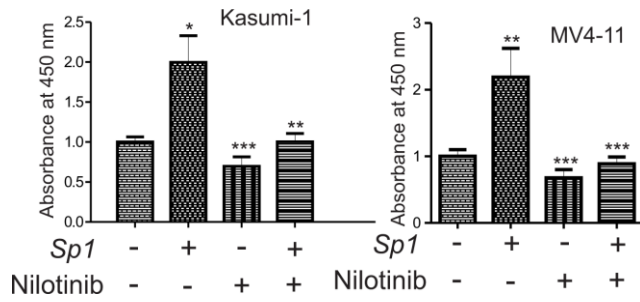
Supplementary Figure 8. *Sp1* overexpression reduces the antileukemia activity of nilotinib. Kasumi-1 and MV4-11 cells were transfected with *Sp1* expression or control vectors for 12 h and then treated with 10 µM nilotinib for another 24 h. CCK-8 assays measuring changes in cell proliferation. Data are shown as mean values ±S.D. and represent six replicates.
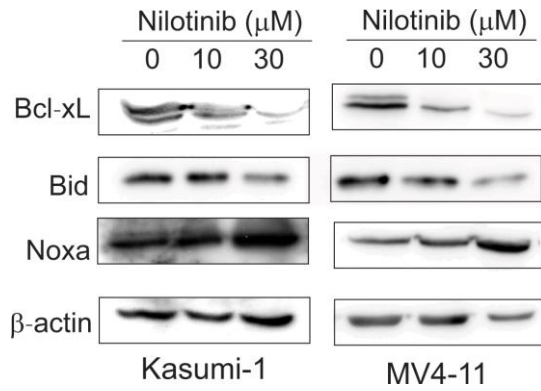
Supplementary Figure 9. Exposure to nilotinib leads to changes in pro- and anti-apoptotic proteins. Kasumi-1 and MV4-11 cells were treated with 10, 30 µM nilotinib for 24 h and subjected to Western blot. Data represent 3 independent experiments.
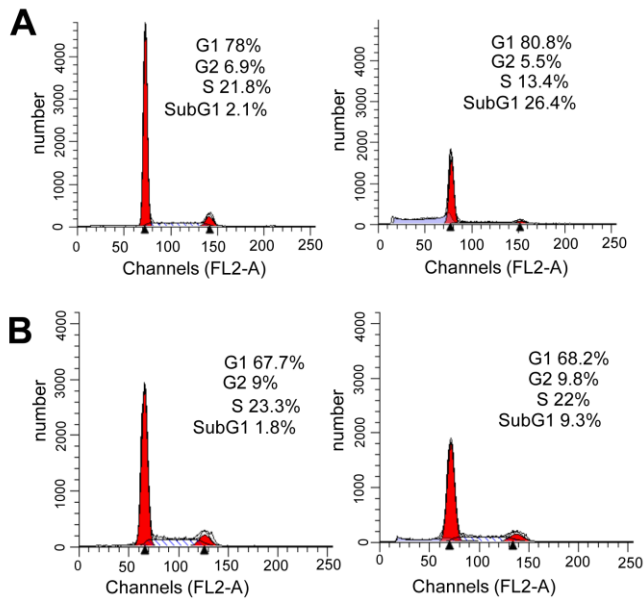
Supplementary Figure 10. Nilotinib treatment displays no obvious changes in cell cycle.

A and **B**, Kasumi-1 (**A**) and MV4-11 (**B**) cells were treated with 30 µM nilotinib for 48 h and subjected to flow cytometry analysis. Representative data from 3 independent experiments that gave similar results are shown.
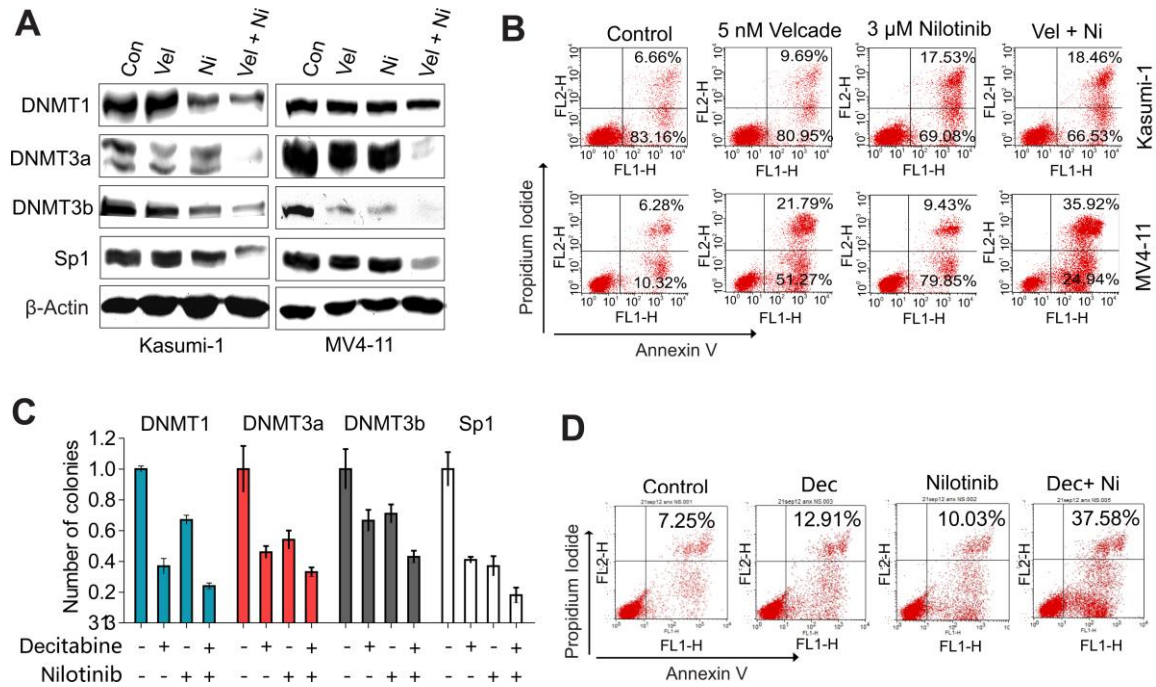
Supplementary Figure 11. Velcade or decitabine sensitizes AML cells to nilotinib treatment.

A and **B**, MV4-11 or Kasumi-1 cells were treated with suboptimal doses of velcade (Vel, 5 nM) or/ and nilotinib (Ni, 3 µM) for 16 hours, and subjected to Western blot analysis to determine protein expression (**A**) and to flow cytometry to measure cellular apoptosis (**B**). **C** and **D**, Kasumi-1 cells were treated with 3 µM nilotinib or/and 1 µM decitabine (Dec) for 6 or 16 h, and subjected to colony-forming assays (6 h, **C**) or flow cytometry analysis (16 h, **D**).
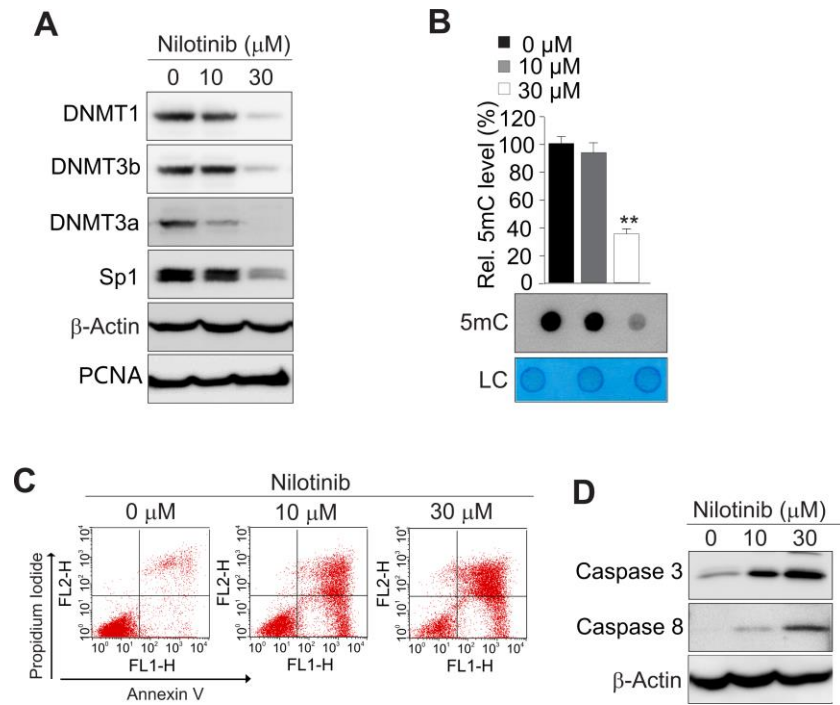
Supplementary Figure 12. Nilotinib exposure induces cell apoptosis through modulation of DNA methylation in the C1498 mouse AML cell line.

A-D, C1498 cells were treated with nilotinib at concentrations of 0, 10 or 30 µM for 24 h and subjected to Western blot analysis (**A,D**), dotblot analysis to detect DNA methylation (**B**) and flow cytometry to measure cellular apoptosis (**C**). In **B**, the graph shows the quantification of dot intensity from 3 independent experiments; LC = loading control; **P <0.01.
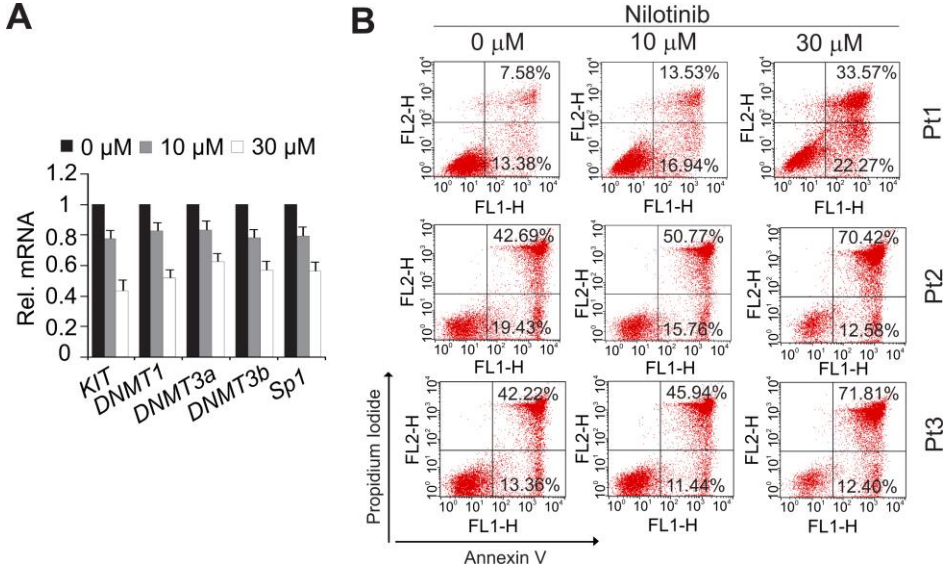
Supplementary Figure 13. Exposure of AML patient primary cells to nilotinib suppresses oncogene expression and promotes cell apoptosis.

A and **B**, PBMCs from AML patients (Pt, n = 3) were treated with nilotinib at concentrations of 0, 10 or 30 µM for 24 h and subjected to qPCR analysis to determine gene expression (**A**) or flow cytometry to measure cellular apoptosis (**B**).
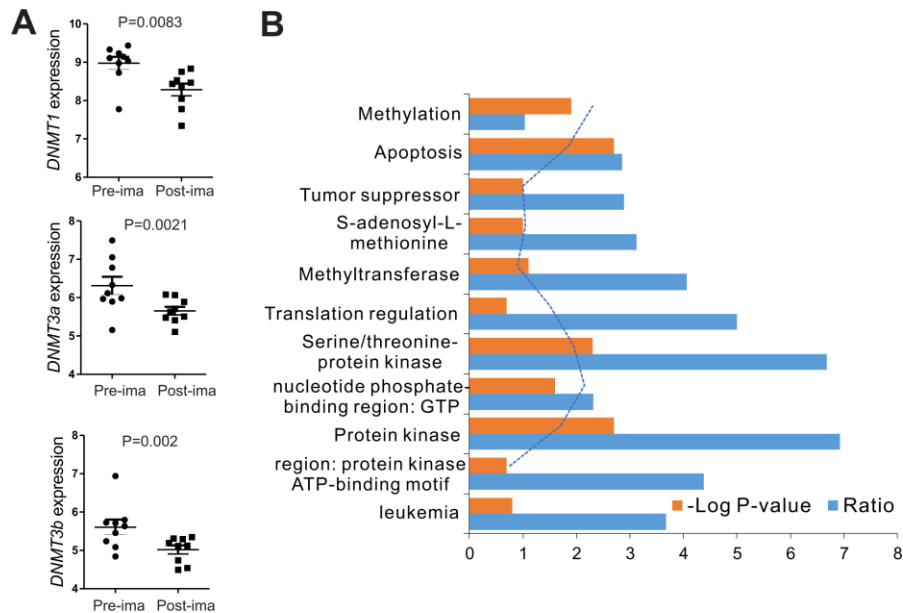
Supplementary Figure 14. The anti-leukemia activities of imatinib involve DNA methylation-associated pathways.

A, GSE33075 analysis for the expression of *DNMT1*, *DNMT3a* and *DNMT3b* in CML patients (n = 9) receiving imatinib therapy. **B**, Enrichment scores for gene ontology categories in the differentially expressed genes described in GSE33075. The –Log (*P* value) axis indicates the statistical significance comparing the functions to the dataset.

Supplementary Table. Primer/probe sequences used in the experiments

The primers for the $p15^{INK4B}$ promoter: forward 5'-GGTTGGTTTT TTATTTTGTTAGAG-3' reverse 5'-ACCTAAACTCAACTTCATTACCCTC-3'
The primers for the *CDH1* promoter: forward 5'-TTTTTTTTGATTTTAGGTTTTAGTGAG-3' reverse 5'-ACTCCAAAAACCCATAACTAACC-3'
The oligo sequences for EMSA: DNMT1/Sp1-1F:5′-GGGCTCCGCGTGGGGGGGGGTGTGTGCCCGCCTTGCGC-3′ DNMT1/Sp1-1R: 5′-GCGCAAGGCGGGCACACACCCCCCCCACGCGGAG-3′
The SYBR Green primers used for qPCR:

The SYBR Green primers used for qPCR:

FLT3	forward 5'-TTGACCAATATGAAGAGTT-3'
	reverse 5'-ATATGCTGTATCCGTTATC-3'
CDH1	forward 5'-AGAACGCATTGCCACATACAC-3'
	reverse 5'-GAGGATGGTGTAAGCGATGG-3'
$p15^{INK4B}$	forward 5'-CCAGATGAGGACAATGAG-3'
	reverse 5'-AGCAAGACAACCATAATCA-3'
p18	forward 5'-ATGGATTTGGAAGGACTG-3'
	reverse 5'-TAGCACCTCTAAGTAGCA-3'
p21	forward 5'-GCGGTTGAATGAGAGGTT-3'
	reverse 5'-AAGGAGAACACGGGATGA-3'
p16	forward 5'-TGGCGGATAGAGCAATGA-3'
	reverse 5'-CGAAAGTCTTCCATTCTTCAAAC-3'
18S	forward 5'-ACAGGATTGACAGATTGA-3'
	reverse 5'-TATCGGAATTAACCAGACA-3'

Supplementary References

1.   Liu S, Wu LC, Pang J, Santhanam R, Schwind S, Wu YZ*, et al.* Sp1/NFkappaB/HDAC/ miR-29b regulatory network in KIT-driven myeloid leukemia. Cancer cell **2010**;17(4):333-47.

2.   Yang X, Pang J, Shen N, Yan F, Wu LC, Al-Kali A*, et al.* Liposomal bortezomib is active against chronic myeloid leukemia by disrupting the Sp1-BCR/ABL axis. Oncotarget **2016**;7(24):36382-94.

3.   Yan F, Shen N, Pang JX, Zhang YW, Rao EY, Bode AM*, et al.* Fatty acid-binding protein FABP4 mechanistically links obesity with aggressive AML by enhancing aberrant DNA methylation in AML cells. Leukemia **2016**;31(6):1434-1442.

4.   Shen N, Yan F, Pang J, Wu LC, Al-Kali A, Litzow MR*, et al.* A nucleolin-DNMT1 regulatory axis in acute myeloid leukemogenesis. Oncotarget **2014**;5(14):5494-509.

5.   Gao XN, Yan F, Lin J, Gao L, Lu XL, Wei SC*, et al.* AML1/ETO cooperates with HIF1alpha to promote leukemogenesis through DNMT3a transactivation. Leukemia **2015**; 29(8):1730-40.

6.   Metzeler KH, Hummel M, Bloomfield CD, Spiekermann K, Braess J, Sauerland MC*, et al.* An 86-probe-set gene-expression signature predicts survival in cytogenetically normal acute myeloid leukemia. Blood **2008**;112(10):4193-201.

7.   Long MD, van den Berg PR, Russell JL, Singh PK, Battaglia S, Campbell MJ. Integrative genomic analysis in K562 chronic myelogenous leukemia cells reveals that proximal NCOR1 binding positively regulates genes that govern erythroid differentiation and Imatinib sensitivity. Nucleic acids research **2015**;43(15):7330-48.

8. Benito R, Lumbreras E, Abaigar M, Gutierrez NC, Delgado M, Robledo C*, et al.* Imatinib therapy of chronic myeloid leukemia restores the expression levels of key genes for DNA damage and cell-cycle progression. Pharmacogenetics and genomics **2012**;22(5):381-8.

9. Asmussen J, Lasater EA, Tajon C, Oses-Prieto J, Jun YW, Taylor BS*, et al.* MEK-dependent negative feedback underlies BCR-ABL-mediated oncogene addiction. Cancer discovery **2014**;4(2):200-15.

10. Bruennert D, Czibere A, Bruns I, Kronenwett R, Gattermann N, Haas R*, et al.* Early in vivo changes of the transcriptome in Philadelphia chromosome-positive CD34+ cells from patients with chronic myelogenous leukaemia following imatinib therapy. Leukemia **2009**;23(5):983-5.

11. Duy C, Hurtz C, Shojaee S, Cerchietti L, Geng H, Swaminathan S*, et al.* BCL6 enables Ph+ acute lymphoblastic leukaemia cells to survive BCR-ABL1 kinase inhibition. Nature **2011**;473(7347):384-8.

12. Neumann F, Teutsch N, Kliszewski S, Bork S, Steidl U, Brors B*, et al.* Gene expression profiling of Philadelphia chromosome (Ph)-negative CD34+ hematopoietic stem and progenitor cells of patients with Ph-positive CML in major molecular remission during therapy with imatinib. Leukemia **2005**;19(3):458-60.

13. Feldhahn N, Henke N, Melchior K, Duy C, Soh BN, Klein F*, et al.* Activation-induced cytidine deaminase acts as a mutator in BCR-ABL1-transformed acute lymphoblastic leukemia cells. The Journal of experimental medicine **2007**;204(5):1157-66.